

Administration.

^(a)Permanent address: Laboratoire de Physique Nucléaire et Hautes Energies, Université Paris VI, Paris, France.

^(b)Present address: DESY, Hamburg, West Germany.

^(c)Permanent address: Laboratori Nazionali, Frascati, Rome, Italy.

^(d)Permanent address: Centre d'Etudes Nucléaires de Saclay, Saclay, France.

¹G. Goldhaber *et al.*, Phys. Rev. Lett. **37**, 255 (1976).

²I. Peruzzi *et al.*, Phys. Rev. Lett. **37**, 569 (1976).

³G. Goldhaber, Bull. Am. Phys. Soc. **22**, 20(T) (1977); G. Goldhaber *et al.*, to be published.

⁴G. J. Feldman *et al.*, Phys. Rev. Lett. **38**, 1313 (1977).

⁵Because charmed mesons are associatively produced by the strong or electromagnetic interaction, and are known to decay weakly [see J. E. Wiss *et al.*, Phys. Rev. Lett. **37**, 1531 (1976)] with parity nonconservation the absolute parity of the D^0 cannot be determined and thus can be set to -1 by convention.

⁶The presence of the decay $D^* \rightarrow D\pi$ implies that the D and D^* have odd relative parity if both are spinless, but then they could not couple to a photon in a P wave without violating parity conservation in electromagnetic production reaction $e^+e^- \rightarrow D^0\bar{D}^{*0}$ or \bar{D}^0D^{*0} . This seems to be one of the dominant production modes for charmed mesons near threshold (see Ref. 3).

⁷The helicity frame is oriented with its z axis (polar axis) along the direction of the D momentum in the over-

all center of mass and its y axis along the production-plane normal.

⁸J. D. Jackson, Lawrence Berkeley Laboratory Internal Note JDJ/76-1 (unpublished).

⁹J.-E. Augustin *et al.*, Phys. Rev. Lett. **34**, 233 (1975).

¹⁰Neutral two-body combinations with both tracks lacking time of flight are dropped from the analysis. This occurs for about 10% of the combinations.

¹¹Background effects were included by the addition of a 15% isotropic background in both production and decay angular distributions. The assumption of background isotropy was checked by background events from 50 MeV/ c^2 sidebands in the $K\pi$ invariant-mass distribution.

¹²The presence of secondary D^{0*} s only slightly distorts the $\cos\Theta$ distribution of Fig. 1(a) because of the small momentum of the D^{0*} s in the D^{*0} rest frame for D^* pion decays.

¹³Errors in the calculation of the expected curves are not included in these χ^2 calculations.

¹⁴We note that there is a 1.5-standard-deviation inconsistency in the widths of the peaks of Fig. 2.

¹⁵S. L. Glashow, I. Iliopoulos, and L. Maiani, Phys. Rev. D **2**, 1285 (1970); A. De Rújula, H. Georgi, and S. L. Glashow, Phys. Rev. D **12**, 147 (1975); M. K. Gaillard, B. W. Lee, and J. L. Rosner, Rev. Mod. Phys. **47**, 277 (1975).

¹⁶G. Altarelli, N. Cabibbo, and L. Maiani, Phys. Rev. Lett. **35**, 635 (1975); S. R. Borchardt and V. S. Mathur, Phys. Rev. Lett. **36**, 1287 (1976).

Nucleus-Nucleus Potential Deduced from Experimental Fusion Cross Sections

R. Bass

Institut für Kernphysik der Universität Frankfurt am Main, 6 Frankfurt, Germany

(Received 16 May 1977)

A classical analysis of recent fusion cross sections is presented. The results are consistent with a schematic model previously published by the author, and allow one to extract an empirical nucleus-nucleus potential.

It has been shown that nucleus-nucleus fusion cross sections can be predicted with remarkable accuracy from simple, classical, two-body models.^{1,2} The basic ingredients of such models are (a) the assumption of a frozen shape of the colliding nuclei during their approach, (b) the assumption of a conservative two-body potential, and (c) the assumption of frictional forces which allow the system to be trapped in a region of attractive interaction.

The validity of this general approach appears to be well established by its success; however, disturbing ambiguities remain with respect to points (b) and (c) above. These can be resolved

only by further careful and systematic comparisons with experimental data. In order to make such a comparison meaningful, fusion excitation functions must be measured with good absolute precision ($\leq 10\%$) over a large range of bombarding energies. Results which meet these requirements have been reported recently for a number of comparatively light nucleus-nucleus systems.³⁻⁸ In the present Letter I examine to what extent these results are consistent with a schematic fusion model¹ and try to deduce an empirical nucleus-nucleus potential.

Following Ref. 1, I define a critical distance $R_{cr} \approx R_{12}$ which marks the onset of strong friction-

al forces ($R_{1/2}$ is the half-density distance). Fusion will then occur for all classical trajectories which penetrate to R_{cr} , provided that the effective conservative (including centrifugal) forces at this point are attractive. With neglect of friction for the limiting trajectory (corresponding to the limiting angular momentum for fusion) at distances $r > r_{fu}$, the classical fusion cross section is given by the well-known relationship

$$E\sigma_{fu} = \pi r_{fu}^2 [E - V(r_{fu})], \quad (1)$$

where r_{fu} is the classical turning point of the limiting trajectory. We note that r_{fu} in general depends on energy and is defined by the condition that the quantity $r^2[E - V(r)]$ be minimized for some $r \geq R_{cr}$, which is then identified as r_{fu} . In order to extract values of r_{fu} and $V(r_{fu})$ from excitation functions, one differentiates Eq. (1) with respect to energy and obtains

$$\begin{aligned} \frac{d}{dE}(E\sigma_{fu}) \\ = \pi r_{fu}^2 - \left(\frac{d}{dr} \{ \pi r^2 [E - V(r)] \} \right)_{r=r_{fu}} \frac{dr_{fu}}{dE}. \end{aligned} \quad (2)$$

It follows from the definition of r_{fu} that the second term on the right-hand side of Eq. (2) is always zero, since r_{fu} is either independent of E ($r_{fu} = R_{cr}$) or minimizes the expression in the curly brackets. Thus one obtains the following equations relating r_{fu} and $V(r_{fu})$ to the experimental data [from Eqs. (1) and (2)]:

$$\pi r_{fu}^2 = d(E\sigma_{fu})/dE, \quad (3)$$

$$V(r_{fu}) = E - \frac{E\sigma_{fu}}{d(E\sigma_{fu})/dE}. \quad (4)$$

These equations can be given a very simple geometrical interpretation, which is shown schematically in Fig. 1(a), and has been used to deduce corresponding pairs r_{fu} , $V(r_{fu})$ from the data given in Refs. 3–8 by a graphical technique. I note, without proof, that a similar method can be applied if σ_{fu} is plotted versus $1/E$, as appears to be popular in the literature [see Fig. 1(b)].

By use of the liquid-drop model and general geometrical arguments, the nuclear part of the nucleus-nucleus potential (for spherical nuclei and frozen densities) can be written as^{1,9,10}

$$-V_n(s) = 4\pi\gamma \frac{R_1 R_2}{R_1 + R_2} f(s) = \frac{R_1 R_2}{R_1 + R_2} g(s), \quad (5)$$

with

$$df/ds = -1 \text{ for } s=0. \quad (6)$$

Here γ denotes the specific surface energy of nu-

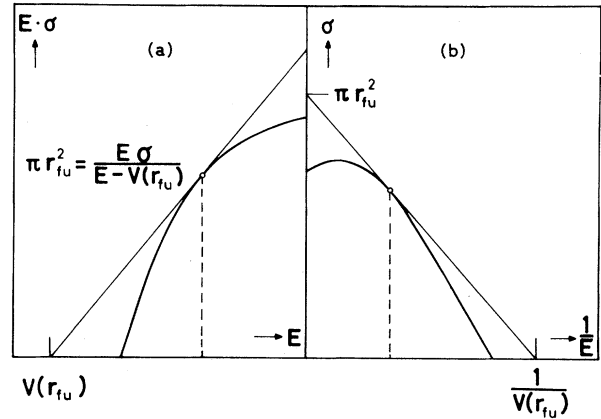


FIG. 1. Classical analysis of excitation functions: (a) plotting $E\sigma$ vs E ; (b) plotting σ vs $1/E$.

clear matter, R_1 and R_2 are suitably defined nuclear radii (see below), and $f(s)$ and $g(s)$ are universal functions of the surface separation coordinate $s = r - R_1 - R_2$. The derivation of Eq. (5) implies that R_1 and R_2 are much larger than the surface thickness and the range of the nuclear force; in this limit, the half-density radius should be the appropriate choice for R . For finite nuclei, R cannot be defined unambiguously without reference to a specific interaction model (see Ref. 10 for a discussion of this point). I write¹¹

$$R = aA^{1/3} - b^2(aA^{1/3})^{-1}, \quad (7)$$

where a is chosen to reproduce half-density-matter radii in the limit of large A , and b is considered adjustable to some extent.

Systematic investigations of various combinations of a and b^2 led to the conclusion that an adequate representation of the fusion data according to Eq. (5) can be obtained with a between 1.12 and 1.16 fm, and b^2 between 1 and 2 fm². Values of a or b^2 significantly outside these limits either appear to be physically unreasonable or result in a distinctly inferior fit to the data. In this paper I adopt $a = 1.16$ fm (following the analysis of Myers¹¹) and—somewhat arbitrarily— $b^2/a = 1.39$ fm (this choice minimizes the scatter of the “experimental” points, but is not sharply defined by the data). It should be noted that the functions $f(s)$ and $g(s)$ deduced from such an analysis depend on the definition of R , and hence on a and b .

“Experimental” points for the function $g(s)$ have been extracted by means of Eqs. (3)–(5) from the fusion cross sections of Refs. 3–8 and are shown in Fig. 2. Following the authors of Refs. 3–7, I have identified their experimental cross sections for evaporation-residue formation with the cor-

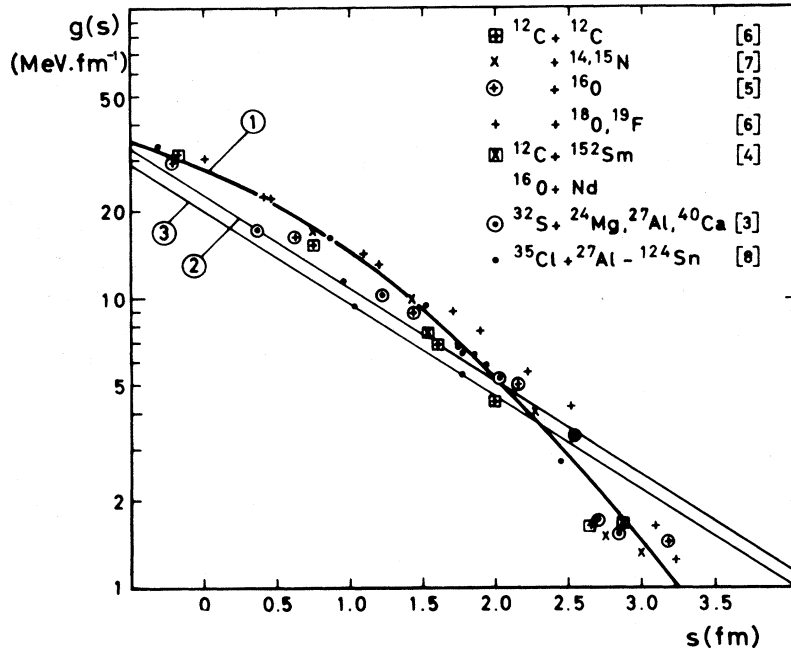


FIG. 2. Nucleus-nucleus potential, expressed in terms of the universal function $g(s)$ as defined in Eq. (5). "Experimental" points from different sources are distinguished by different symbols, and the corresponding references are given. Curve 1 is a fit to the data according to Eq. (8). The straight lines marked 2 and 3 represent the potential from Ref. 1 (line 2, $\tau_0 = 1.00$ fm; line 3, $\tau_0 = 1.07$ fm).

responding cross sections for complete fusion, thus neglecting the possibility of compound-nucleus decay by fission. From a literature survey of existing experimental and theoretical information on compound systems of comparable mass and charge one may conclude that the fission channel should account for less than 5% of the total fusion cross section for the systems and energy ranges considered. Measured fusion-fission contributions of less than 10% (and with almost negligible effect on the results of the present analysis) are included in the cross sections for ^{35}Cl -induced fusion reactions taken from Ref. 8. Oscillations with relative amplitudes of the order of 10–20%, which occur in the experimental excitation functions for the systems $^{12}\text{C} + ^{12}\text{C}$ (Ref. 6) and $^{12}\text{C} + ^{16}\text{O}$ (Ref. 5), have been smoothed prior to analyzing the data.

Each point in Fig. 2 is associated with correlated uncertainties in s and $g(s)$, which depend on the absolute accuracy and energy range of the experimental cross sections, and on the ratio of the Coulomb potential to the nuclear potential for the system and separation involved. The resulting error is less than $\pm 25\%$ in $g(s)$ (projected for constant s) or less than ± 0.25 fm in s [projected for constant $g(s)$] in all cases. In general, the

results for different systems are in remarkable agreement, and hence confirm the predicted universal behavior of the function $g(s)$. The data can be fitted with an empirical function of the form

$$g(s) = [A \exp(s/d_1) + B \exp(s/d_2)]^{-1}, \quad (8)$$

where $A = 0.0300 \text{ MeV}^{-1} \text{ fm}$, $B = 0.0061 \text{ MeV}^{-1} \text{ fm}$, $d_1 = 3.30 \text{ fm}$, and $d_2 = 0.65 \text{ fm}$, which is included in Fig. 2. Disregarding inaccuracies in the experimental data and in the present analysis, the scatter of the points around the fitted curve could be explained entirely as due to small fluctuations (typically less than ± 0.3 fm) of $R_1 + R_2$ around the average trend as given by Eq. (7). One notes further that the empirical potential [Eq. (8)] approximately satisfies Eq. (6).

For comparison, I also show in Fig. 2 $g(s)$, as deduced from the potential given in Ref. 1

$$\begin{aligned} -V_N(s) &= \frac{da_s A_1^{1/3} A_2^{1/3}}{R_1 + R_2} \exp\left(-\frac{s}{d}\right) \\ &\approx \frac{da_s}{r_0^2} \frac{R_1 R_2}{R_1 + R_2} \exp\left(-\frac{s}{d}\right), \end{aligned} \quad (9)$$

where $d = 1.35 \text{ fm}$ and $a_s = 17 \text{ MeV}$. Since the first part of Eq. (7) does not scale exactly as $R_1 R_2 / (R_1 + R_2)$, a comparison with the present analysis

in terms of Eq. (5) involves an assumption on the average radius parameter $r_0 = R/A^{1/3}$. The two straight lines shown in Fig. 2 correspond to $r_0 = 1.00$ fm (appropriate to light nuclei) and $r_0 = 1.07$ fm (approximate average for all mass numbers), respectively. Evidently the simple exponential potential of Ref. 1 reproduces the empirical-fit function quite well on the average, but falls off too slowly at large distances.

Christensen and Winther¹² have recently performed a global analysis of heavy-ion elastic scattering data, based on semiclassical arguments and the recognition that optical-model analyses of elastic scattering determine the real part of the potential only in the vicinity of a characteristic distance. Corresponding values of distance and potential were deduced for a large number of systems and bombarding energies, and were found consistent with Eq. (5) (using, however, somewhat different parameters a and b). The same set of potential and distance values is very well reproduced by the present empirical fusion potential as given by Eq. (7), with a deviation of less than $\pm 25\%$ in $g(s)$ or less than ± 0.2 fm in s in about 80% of all cases. The relevant range of s values (as calculated with my parameters a and b) goes from about 3 to 4.5 fm, and thus extends the range covered by the fusion data towards larger values.

In conclusion, I have derived a universal nucleus-nucleus potential from a classical analysis of experimental fusion cross sections. The deduced potential is consistent with the liquid-drop model at small separation, and with quantal analyses of elastic scattering at large separation. I emphasize that the present analysis is based on the assumption of negligible dissipation (friction) at distances larger than the critical distance, at least

for the limiting trajectory. Should this assumption be invalid, then the present potential has no physical significance. However, the remarkable consistency of the results for many systems and energies among one another and with theoretical predictions gives, in my opinion, strong indirect evidence in favor of weak long-range dissipation (but strong short-range dissipation). I therefore suggest that the assumption of strong frictional forces at large separation² is an artifact of fitting deep inelastic scattering with unrealistic potentials and/or neglecting essential degrees of freedom.

¹R. Bass, Phys. Lett. **47B**, 139 (1973), and Nucl. Phys. **A231**, 45 (1974).

²D. H. E. Gross and H. Kalinowski, Phys. Lett. **48B**, 302 (1974); D. H. E. Gross, H. Kalinowski, and J. N. De, in *Proceedings of the 1974 Heidelberg Symposium on Classical and Quantum Mechanical Aspects of Heavy Ion Collisions*, edited by H. L. Harney *et al.* (Springer, Berlin, 1975), p. 194.

³H. H. Gutbrod, W. G. Winn, and M. Blann, Nucl. Phys. **A213**, 267 (1973).

⁴R. Broda *et al.*, Nucl. Phys. **A248**, 356 (1975).

⁵P. Sperr *et al.*, Phys. Rev. Lett. **36**, 405 (1976).

⁶P. Sperr *et al.*, Phys. Rev. Lett. **37**, 321 (1976).

⁷M. Coujeaud *et al.*, in *Proceedings of the European Conference on Nuclear Physics with Heavy Ions*, Caen, France, 6–10 September 1976 (unpublished).

⁸W. Scobel *et al.*, Phys. Rev. C **14**, 1808 (1976).

⁹J. Wilczynski, Nucl. Phys. **A216**, 386 (1973).

¹⁰J. Randrup, W. J. Swiatecki, and C. F. Tsang, Lawrence Berkeley Laboratory Report No. 3603, 1974 (to be published); J. Blocki *et al.*, Lawrence Berkeley Laboratory Report No. 5014, 1976 (to be published).

¹¹W. D. Myers, Nucl. Phys. **A204**, 465 (1973).

¹²R. Christensen and A. Winther, Phys. Lett. **65B**, 19 (1976).